Investigating the Kinematics of the Di-Higgs Signal in the 0-lepton $bbWW^*$ Channel with the ATLAS Detector at LHC

Shiksha Pandey, *Bryn Mawr College, Pennsylvania*
Supervisors: Harris Kagan, Shaun Roe, Suyog Shrestha

Abstract
The study of the production and decay of di-Higgs in various channels is important to better understand the nature of the Higgs bosons and to check the validity of the Standard Model. Here, we investigate the $HH \to bbWW^* \to bbqqqq$ channel to determine suitable triggers and to identify the on and off-shell W bosons that subsequently decay into four light quarks. From the initial study, various prospective cuts for triggers have been determined. Additionally, a correspondence between the mass and the transverse momentum of the W bosons for four-fifths of the total events has been observed, and the off-shell W has been identified as the one with lower transverse momentum for most events.

Keywords
di-Higgs, all hadronic, kinematics, transverse momentum, off-shell, trigger

1 Introduction

The observable matter is made up of fermions or matter particles, the gauge bosons or the force carrying particles, and the Higgs boson. Their interactions are governed by the four forces in nature: the weak force, the strong force, the electromagnetic force and the gravitational force. The Standard Model (SM) of particle physics is a framework that describes these fundamental particles and the forces except for gravity. In the SM, elementary particles acquire mass as a result of their interaction with the Higgs field, which is a scalar field associated with the Higgs boson–a neutral spin-0 particle of mass 125 GeV [1].

The SM is an extremely precise theory; the experimental results so far have been in agreement with the predictions of the SM. However, it still can't encapsulate gravity into the framework, nor can it explain neutrino mass. In addition, dark matter and dark energy–which make up about 27% and 68% of the universe, respectively, aren't incorporated in the SM. Thus, it is clear that the SM isn't a complete theory. In order to tackle the open questions that the SM cannot explain, it is imperative that we better our understanding of the fundamental particles and their interactions, and look for deviations from the SM. One area of focus to probe into the limitations of the SM is the measurement of the self-coupling of the Higgs boson, which remains a major goal of the Large Hadron Collider (LHC) at CERN. The direct measurement of the self-coupling of the Higgs boson can be done by measuring the di-Higgs production cross section, and it is possible that the value of the self-coupling of the Higgs boson may deviate from the SM predictions. Thus, di-Higgs production and various decay channels have been studied extensively.

Figure 1 shows two most dominant modes of the pair production of the Higgs boson. Gluons in proton-proton collision fuse to give two Higgs bosons via square or triangular top quark loops. In the second diagram in Figure 1, the interaction of three Higgs bosons at a single vertex can be seen, which is called the trilinear coupling (λ_{hhh}).

The pair of Higgs bosons thus produced can decay through various channels such as $HH \to bbbb$, $HH \to bbVV$, $HH \to VVVV$, $HH \to bb\tau\tau$, $HH \to bb\gamma\gamma$, where V represents the vector bosons W and Z. In this paper, we focus on the $HH \to bbWW \to bbqqqq$ 0-lepton channel, which has not been published prior to this.

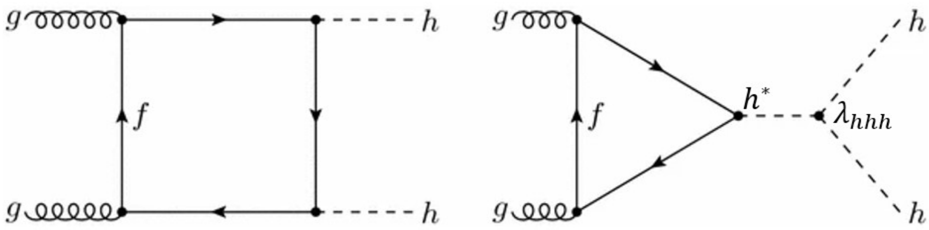

Figure 1: Leading order feynmann diagrams for the pair production of the Higgs boson via gluon-gluon fusion

2 The Large Hadron Collider

Figure 2 shows a part of the Large Hadron Collider (LHC). The most powerful and the largest particle accelerator in the world, the LHC has a 27 Km ring where proton beams coming from opposite directions at speeds close to that of light are made to collide. The particle beams travel inside the beam pipes in the collider tunnel. The ring consists of superconducting magnets along with other accelerating structures that boost the energy of the particle beams. Many superconducting electromagnets are present to guide the proton beams in desired directions. The CERN control centre then makes the collisions happen at locations corresponding to the ATLAS, ALICE, LHCb, and CMS detectors that are the part of the accelerator complex at LHC. Near the collision points, stronger electromagnets are used in order to maximize the chances that the beams will intersect.

Figure 2: The Large Hadron Collider at CERN

Per second, a beam of 100 billion protons are collided 25 million times in the LHC. A very small fraction of them contribute to proton-proton collisions [2]. The luminosity [1] of LHC is $2.06 \times 10^{34} cm^{-2} s^{-1}$ as of 2017 [3].

[1]Luminosity is the measure of the number of particle collisions that take place inside the collider. It doesn't give an exact number, rather it is the ratio of the number of events per time to the cross section.

3 The ATLAS Detector

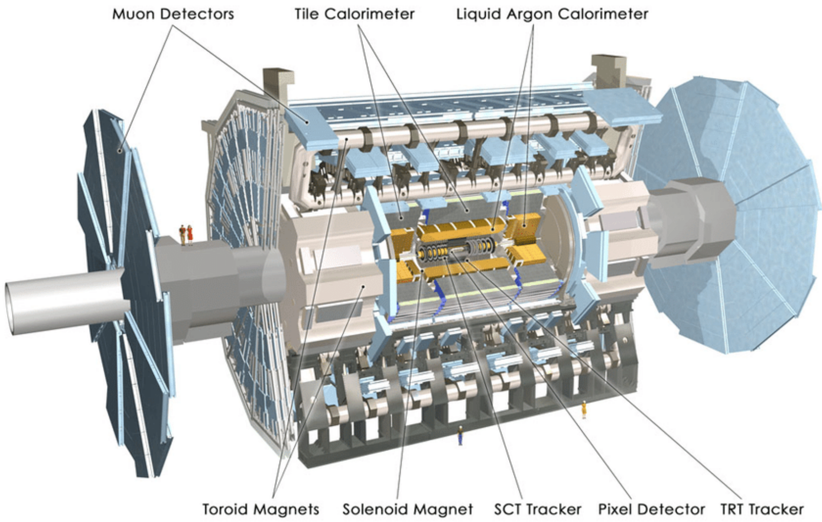

Figure 3: Schematic of the ATLAS detector [4]

ATLAS is one of the two general purpose detectors at LHC, the other being CMS. It is used for Higgs precision measurements along with the search for new physics and other studies. The proton beams are made to collide at the centre of ATLAS, from which the decay products fly off in different directions and are detected at various sub-detectors inside ATLAS. These sub-detectors are arranged in layers to record the energy, momenta, and paths of the particles. In particle collisions, a lot of data is produced and not all of it will be relevant. To selectively record the relevant data, ATLAS uses advanced trigger systems.

The ATLAS detector has four main components: the Inner Detector, the Calorimeters, the Muon Spectrometer, and the Magnet System. The magnet system is made up of various solenoid and torroidal magnets that bend the particle trajectories around different layers of the detector system [5]. The innermost portion, the Inner detector, consists of the pixel detector, silicon tracker, and transition radiation tracker. In this highly sensitive area, particle trajectories and collision vertices are reconstructed, and the momenta and charges of electrically charged particles are measured [6]. The next component consists of two types of calorimeters: the electromagnetic calorimeter for measuring the energy deposited by particles that interact electromagnetically such as the photon and the electron, and the hadronic calorimeter for measuring the energy of the hadrons [7]. The outermost layer of the ATLAS detector is the Muon spectrometer that detects the muons which pass through the inner detector and the calorimeters undetected [8]. A neutrino passes through all the layers of the ATLAS detector without being detected. The missing energy associated with a neutrino or other particles that escape without detection contributes to the missing transverse energy.

4 Methods

The Signal event of interest involves the pair production of Higgs bosons where one decays into two b quarks, and the other decays into two W bosons each of which decay into 2 light quarks as shown in Figure 4. The events were generated using Monte Carlo simulation with the assigned mass of the Higgs Boson $m_H = 125$ GeV, at the center of mass energy $\sqrt{s} = 13$ TeV. The resultant recorded quantities were the transverse momenta, mass, pseudo rapidity, and azimuthal angles of the light and b-quarks. Utilizing them, various kinematic plots were analyzed and the masses of the W bosons were reconstructed.

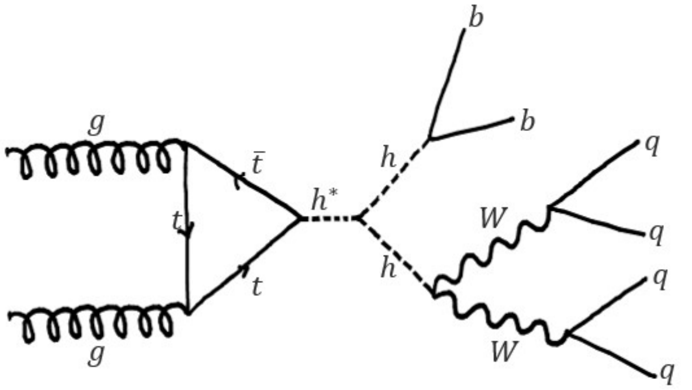

Figure 4: A schematic diagram of the di-Higgs production and decay process

5 Results and Discussion

5.1 Cuts for Trigger

Figure 5 shows the distributions for the transverse momenta of the final decay products. They were sorted in descending order of the transverse momentum for each event. The distributions are normalized.

Based on the distribution, various selection cuts for trigger were determined that can be employed to potentially improve the sensitivity of the signal. The results are presented in Table 1.

Table 1 Selection cuts for Trigger

Cuts	Trigger Efficiency
$q1pT > 40$ GeV	97 $\%$
$q2pT > 20$ GeV	97 $\%$
$q3pT > 10$ GeV	96 $\%$
$q4pT > 2.5$ GeV	96 $\%$
$b1pT > 64$ GeV	96 $\%$
$b2pT > 12$ GeV	96 $\%$
$b1pT > 35$ GeV, $q1pT > 35$ GeV, $q2pT > 30$ GeV, and $q3pT > 25$ GeV	84 $\%$
$b1pT > 55$ GeV, $b2pT > 35$ GeV, $q1pT > 35$ GeV, and $q2pT > 30$ GeV	86 $\%$

These cuts can help include only the interesting events and discard the others along with background interference to a certain degree. However, values less than 20 GeV are too small for experiments done at such high energies, and hence, not particularly helpful. So when we put the cut off as 20 GeV for q3, q4, and b2, the following trigger efficiencies were found:

Table 2 Selection cuts for Trigger

Cuts	Trigger Efficiency
$q3pT > 20$ GeV	72 $\%$
$q4pT > 20$ GeV	21 $\%$
$b2pT > 20$ GeV	88 $\%$

The trigger efficiency of $q4pT > 20$ GeV = 21 percentage is too low, so it's best not to include it in our trigger system. Alternatively, 20 GeV is too high a threshold for us to include all our singal.

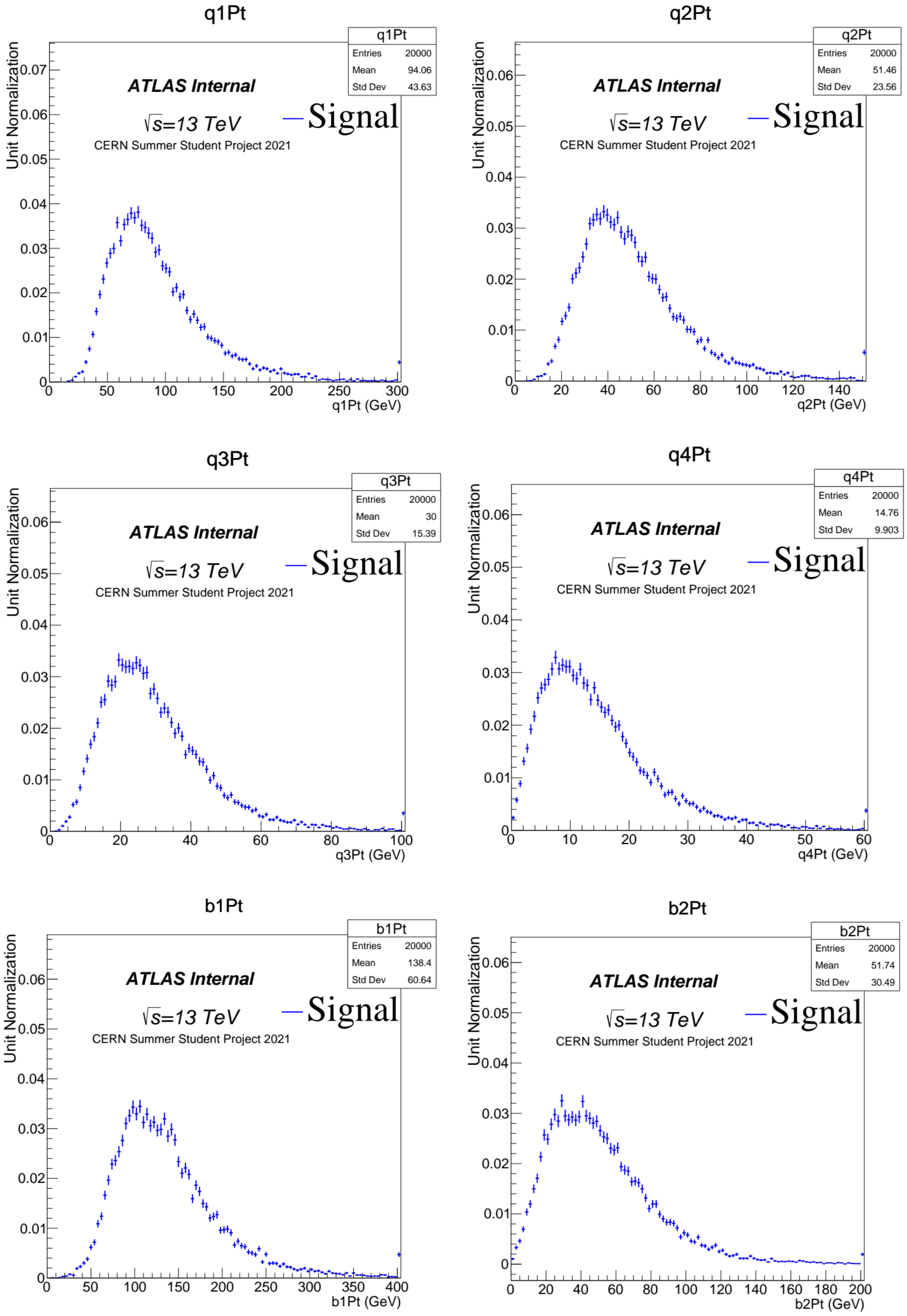

Figure 5: Normalized transverse momenta distributions of the final decay products

5.2 Kinematics of the W Boson

In all channels, the W bosons are intermediate products, so they can't be directly detected. However, they can be reconstructed based on their decay products. Figure 6 shows the transverse momenta of the W bosons, and Fig. 7 shows the mass distribution for the same. In the second distribution in Fig. 7, two peaks can be seen: one at 80 GeV which is the mass of the on-shell W boson [9], and another near 40

GeV. The peak at 40 GeV corresponds to the off-shell W boson [2].

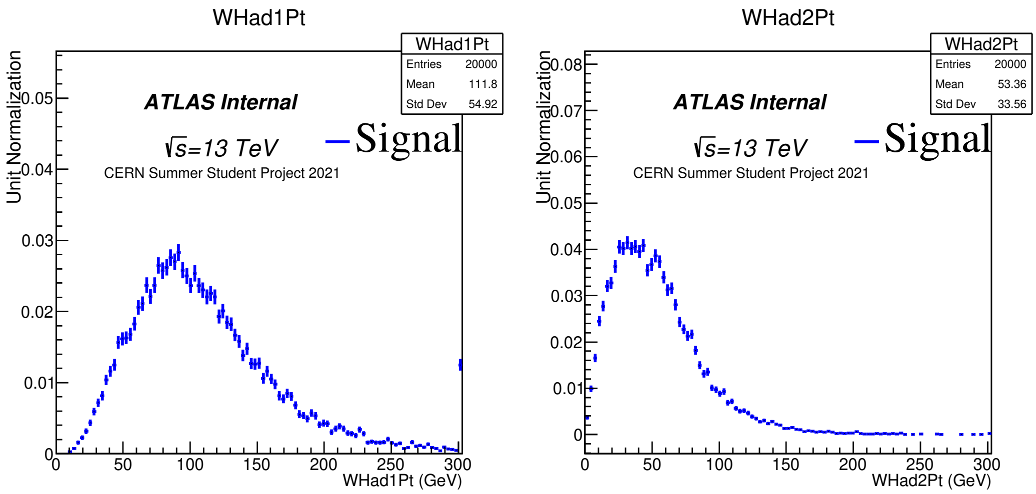

Figure 6: Normalized distributions of the transverse momenta of the W bosons

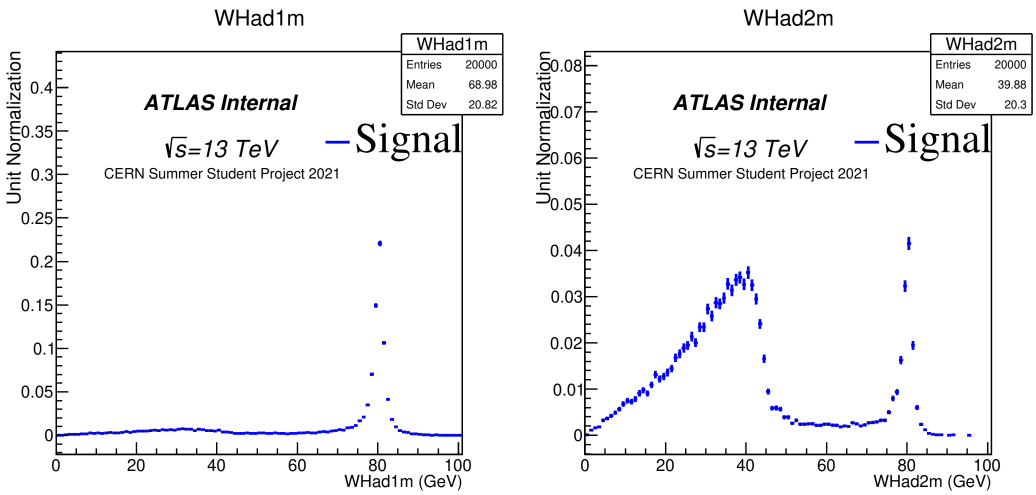

Figure 7: Normalized mass distributions of the W bosons

In this analysis, a correspondence was seen between the mass and the pT of the W bosons. It was observed that the W boson with higher mass also had a higher pT for 80 % of the total events. Moreover, the W boson with a lower pT was almost always the off-shell W; 84% of the time, the lower pT W had a mass < 70 GeV.

One of the objectives of this study was to determine which quarks come from which W boson. Instead of a specific combination of quarks for all events, varied combinations of quarks seemed to result from the W bosons for different events as shown in Table 3; the quarks with the first and the second

[2]Off-shell or virtual particles temporarily violate the energy momentum relation $m^2c^4 = E^2 - p^2c^2$. They have a mass different from the ordinary (also called real or on-shell) particle; the closer the mass of the off-shell particle is to that of the ordinary particle, the longer it takes to decay. Virtual particles are represented by the internal lines of the Feynman diagram. [10]

highest pTs weren't always the decay products of the higher pT W.

Table 3 The mass reconstruction of the W boson with leading pT

The decay results	Number of events
$q1, q2$	6478
$q1, q3$	2789
$q1, q4$	3501
$q2, q3$	2895
$q2, q4$	2895
$q3, q4$	1823

Here, the number of events represents the number of events for which the sum of the masses of the quarks was within 10 GeV of the mass of the W boson with leading pT. The reason we used $WHad1_m - (q_i + q_j).m() = \pm 10$ GeV instead of $WHad1_m = (q_i + q_j).m()$, where $1 \leq i, j \leq 4$ and $i \neq j$, is:

$i)$ The mass of the W boson $\neq$ the sum of the masses of the decay products, i.e., $m(W) \neq m(q_i + q_j)$.

$ii)$ Given $m(W_1) \rightarrow m(W_2) \rightarrow \cdots \rightarrow m(W_n),\ m(W_1) \neq m(W_n)$ in the numerical history of the MC generator.

While that decision to include events within 10 GeV of the mass of W boson with higher pT makes our study more practical, it also counts a few events more than once and because of that, the number of events in Table 3 add up to 20,381–which is larger than the actual number of events = 20000.

6 Conclusion

The study of the kinematics of the products of di-Higgs decay provide valuable insight into suitable triggers, and also inform us about the reconstruction of the intermediate products. In this decay channel: $HH \rightarrow bbWW \rightarrow bbqqqq$, an off-shell W is present. In addition, the higher mass W is found to have a higher pT for four-fifths of the total events, and the lower pT event is found to correspond to the off-shell W for 84% of the total events. There doesn't seem to be a conclusive relationship between the W boson with the higher pT and the two quarks with the leading pTs.

In the future, the studied cuts for trigger can be compared to the ones already available at ATLAS and be used in the design of new triggers. Moreover, the study conducted is a truth level experiment, and the detector level studies will be much more complicated. Hence, it can be checked whether the analysis of the on and off-shell W still hold in the detector level.

Acknowledgements

I would like to express my sincere gratitude to Dr. Suyog Shrestha for his guidance and supervision, Dmitriy Zubov for generating the Monte Carlo events for HH, and CERN summer program for providing me with this opportunity.

Bibliography

[1] G. Aad et al.(ATLAS Collaboration), Physical Review D 90, 052004 (2014).

[2] Illuminating! Couting LHC Collisions with CMS, available at https://cms.cern/news/illuminating-counting-lhc-collisions-cms.

[3] Record Luminosity: Well done LHC, available at https://home.cern/news/news/accelerators/record-luminosity-well-done-lhc.

[4] R. Reed, Journal of Physics Conference Series 1742-6588. 623. 10.1088/1742-6596/623/1/012024 (2014).

[5] Magnet System, available at https://atlas.cern/discover/detector/magnet-system.

[6] The Inner Detector , available at https://atlas.cern/discover/detector/inner-detector.

[7] Calorimeters, available at https://atlas.cern/discover/detector/calorimeter.

[8] Alligning the Muon Spectrometer, available at https://home.cern/news/news/experiments/aligning-atlas-muon-spectrometer.

[9] The ATLAS Collboration, European Phys. J. C 78 (2018) 110 http://dx.doi.org/10.1140/epjc/s10052-017-5475-4

[10] G.Jaeger, Entropy 2019, 21, 141. https://doi.org/10.3390/e21020141